The Astronomical Journal, 144:148 (10pp), 2012 November doi:10.1088/0004-6256/144/5/148

SPITZER PHOTOMETRY OF *WISE*-SELECTED BROWN DWARF AND HYPER-LUMINOUS INFRARED GALAXY CANDIDATES

Roger L. Griffith[1], J. Davy Kirkpatrick[1], Peter R. M. Eisenhardt[2], Christopher R. Gelino[1], Michael C. Cushing[3], Dominic Benford[4], Andrew Blain[5], Carrie R. Bridge[6], Martin Cohen[6], Roc M. Cutri[1], Emilio Donoso[1], Thomas H. Jarrett[1], Carol Lonsdale[8], Gregory Mace[9], A. Mainzer[2], Ken Marsh[10], Deborah Padgett[4], Sara Petty[9], Michael E. Ressler[2], Michael F. Skrutskie[11], Spencer A. Stanford[12], Daniel Stern[2], Chao-Wei Tsai[1], Edward L. Wright[9], Jingwen Wu[2], and Lin Yan[1]

[1] Infrared Processing and Analysis Center, California Institute of Technology, Pasadena, CA 91125, USA
[2] Jet Propulsion Laboratory, California Institute of Technology, 4800 Oak Grove Dr., Pasadena, CA 91109, USA
[3] Department of Physics and Astronomy, MS 111, University of Toledo, 2801 W. Bancroft St. Toledo, OH 43606-3328, USA
[4] NASA Goddard Space Flight Center, Greenbelt, MD 20771, USA
[5] Department of Physics and Astronomy, University of Leicester, LE1 7RH Leicester, UK
[6] Department of Astrophysics, California Institute of Technology, Pasadena, CA 91125, USA
[7] Monterey Institute for Research in Astronomy, 200 8th Street, Marina CA 93933, USA
[8] National Radio Astronomy Observatory, 520 Edgemont Road, Charlottesville, VA 22903, USA
[9] Astronomy Department, University of California Los Angeles, P.O. Box 951547, Los Angeles, CA 9009, USA
[10] School of Physics and Astronomy, Cardiff University, Cardiff CF24 3AA, UK
[11] Department of Astronomy, University of Virginia, Charlottesville, VA 22904, USA
[12] Department of Physics, University of California Davis, One Shields Avenue, Davis, CA 95616, USA
Received 2012 August 2; accepted 2012 September 8; published 2012 October 11

ABSTRACT

We present *Spitzer* 3.6 and 4.5 μm photometry and positions for a sample of 1510 brown dwarf candidates identified by the *Wide-field Infrared Survey Explorer* (*WISE*) all-sky survey. Of these, 166 have been spectroscopically classified as objects with spectral types M(1), L(7), T(146), and Y(12). Sixteen other objects are non-(sub)stellar in nature. The remainder are most likely distant L and T dwarfs lacking spectroscopic verification, other Y dwarf candidates still awaiting follow-up, and assorted other objects whose *Spitzer* photometry reveals them to be background sources. We present a catalog of *Spitzer* photometry for all astrophysical sources identified in these fields and use this catalog to identify seven fainter (4.5 μm $\sim$ 17.0 mag) brown dwarf candidates, which are possibly wide-field companions to the original *WISE* sources. To test this hypothesis, we use a sample of 919 *Spitzer* observations around *WISE*-selected high-redshift hyper-luminous infrared galaxy candidates. For this control sample, we find another six brown dwarf candidates, suggesting that the seven companion candidates are not physically associated. In fact, only one of these seven *Spitzer* brown dwarf candidates has a photometric distance estimate consistent with being a companion to the *WISE* brown dwarf candidate. Other than this, there is no evidence for any widely separated (>20 AU) ultra-cool binaries. As an adjunct to this paper, we make available a source catalog of $\sim$7.33 $\times 10^5$ objects detected in all of these *Spitzer* follow-up fields for use by the astronomical community. The complete catalog includes the *Spitzer* 3.6 and 4.5 μm photometry, along with positionally matched B and R photometry from USNO-B; J, H, and K_s photometry from Two Micron All-Sky Survey; and $W1$, $W2$, $W3$, and $W4$ photometry from the *WISE* all-sky catalog.

Key words: brown dwarfs – galaxies: evolution – galaxies: high-redshift – galaxies: photometry

Online-only material: color figures, supplemental data (FITS) file

1. INTRODUCTION

In the historical nomenclature of stellar classification, astronomers have classified stars according to their spectra, finally settling on the following spectral types, OBAFGKM, with O representing the hottest stars and M the coolest (Morgan et al. 1943). With the discovery of numerous (sub)stellar objects cooler than the coldest M dwarfs, the need for new spectral types became evident. To describe and characterize this new population, two new spectral types were introduced to the stellar taxonomy, L and T dwarfs (see, e.g., Kirkpatrick 2005 for an in depth review), while a new type, "Y," is used for even colder objects, as suggested by Kirkpatrick et al. (1999) and Kirkpatrick (2000).

These low-mass, low-temperature astrophysical sources are considered to be the lowest-mass population of star-like objects. Those with masses below $\sim$0.075 $M_{\odot}$ are referred to as "brown dwarfs"(Kumar 1963; Hayashi & Nakano 1963) and have core temperatures insufficient to sustain hydrogen fusion. Brown dwarfs are important objects for several reasons. They provide benchmarks with which to test our theories of gas chemistry and cloud formation in low-temperature atmospheres (Burgasser 2008). As analogs of extra-solar planets, brown dwarfs are easier to study because they are typically isolated. They represent in situ time capsules of star formation, since their mass is never recycled back into the interstellar medium, therefore preserving information on metallicity enrichment over the lifetime of the Galaxy (Burgasser 2008). They provide important constraints on both the functional form of the stellar mass function and the low-mass limit of star formation (Kirkpatrick et al. 2012; Metchev et al. 2008; Reylé et al. 2010; Burningham et al. 2010). Though predicted to exist in the 1960s, brown dwarfs remained elusive for decades until surveys such as the Two Micron All-Sky Survey (2MASS; Skrutskie et al. 2006), the Sloan Digital Sky Survey (York et al. 2000), and the Deep Near-Infrared Survey of the Southern Sky (DENIS; Epchtein et al. 1997) revealed them in large numbers.

Recently, researchers have shifted their focus toward the coldest brown dwarfs, which are one of the two primary science objectives of the *Wide-field Infrared Survey Explorer* (*WISE*; Wright et al. 2010). *WISE* launched on 2009 December 14 and began surveying the sky on 2010 January 7 at wavelengths of 3.4, 4.6, 12, and 22 μm, hereafter referred to as $W1$, $W2$, $W3$, and $W4$, respectively. It completed its first full pass of the sky on 2010 July 17 and the *WISE* All-Sky Data Release was issued on 2012 March 14.[13] The survey reaches 5σ point source sensitivities in unconfused regions to better than 0.08, 0.11, 1 and 6 mJy, respectively (Wright et al. 2010). The $W1$ and $W2$ filters were specifically designed to probe the deep 3.3 μm CH_4 absorption band in the spectra of brown dwarfs and the region relatively free of opacity at $\sim$4.6 μm, making their $W1 - W2$ colors very red and allowing cool brown dwarfs to be readily identifiable.

Hundreds of potentially ultra-cool brown dwarf candidates have been identified using the *WISE* All-Sky Data. A detailed description of this search is described in Kirkpatrick et al. (2011, 2012), where, along with Mainzer et al. (2011), Wright et al. (2011), Burgasser et al. (2011), Cushing et al. (2011), Gelino et al. (2011), and G. Mace et al. (in preparation), follow-up and preliminary analyses have been presented. With the relatively shallow depth of *WISE*, a majority of these ultra-cool brown dwarf candidates either have very faint $W1$ detections or were simply not detected in $W1$, resulting in $W1 - W2$ color limits. The *Spitzer* Infrared Array Camera (IRAC) 3.6 and 4.5 μm bands (Fazio et al. 2004), sometimes referred to as $ch1$ and $ch2$, are very similar to the $W1$ and $W2$ filters in *WISE*. This makes IRAC an excellent instrument for deeper follow-up observations (see Figure 2 in Mainzer et al. 2011).

In this paper, we present the photometric properties from IRAC follow-up of a large sample ($\sim$1500) of *WISE*-selected brown dwarf candidates (see Section 4.1). Of these, 182 have been spectroscopically classified, with classifications ranging from a single M dwarf to 12 examples of the latest and coldest spectral type, Y (Kirkpatrick 2008; Cushing et al. 2011; Kirkpatrick et al. 2012). We also present new, ultra-cool brown dwarf candidates discovered using the *Spitzer* data alone in an effort to identify fainter, widely separated companions to the *WISE* sources. As a control sample, we also identify field brown dwarf candidates from a *Spitzer* campaign to follow-up *WISE*-selected hyper-luminous infrared galaxy (HyLIRG) candidates (see Section 4.2), as this enables us to assess whether the *Spitzer*-selected brown dwarf companion candidates are more likely to be truly associated with the *WISE*-selected brown dwarf candidates. We release a catalog for 906 *WISE*-selected HyLIRG candidates. In addition to these two extremely rare populations of astrophysical sources, we release a photometric catalog of $\sim 7.33 \times 10^5$ sources detected in the 1000's of *Spitzer* Astronomical Observation Requests (AORs) in these follow-up campaigns. In Section 2, we briefly describe the observations. We discuss the photometry and source detection in Section 3. In Section 4, we describe the catalogs presented in this release. We discuss the new brown dwarf candidates discovered by this analysis in Section 5 and summarize the paper in Section 6. All magnitudes are given in the Vega system unless otherwise noted.

2. OBSERVATIONS

Warm *Spitzer* observations were carried out at 3.6 and 4.5 μm under *Spitzer* programs 70062, 70162, 80033, and 80109. Both the brown dwarf and HyLIRG candidate field observations used a 5-point dither pattern with 30 s exposures per pointing in each IRAC band. IRAC has a $5' \times 5'$ field of view with $1\farcs2$ pixels. For this analysis, we utilized the post-BCD *Spitzer* pipeline images, which have been resampled onto $0\farcs6$ pixels. The AORs were executed between 2010 June and 2012 May and comprise a total of 1564 brown dwarf and 919 extragalactic follow-up observations. These observations have been described in detail in Kirkpatrick et al. (2011) and Eisenhardt et al. (2012). The images for this analysis were reduced with two different versions of the *Spitzer* reduction pipeline, 18.18 and 19.1, with the only change between the two versions being an update to the masking process which includes knowledge of latents going back to previous AOR's. None of these changes affect our reduction and processing techniques.

3. DETECTION AND PHOTOMETRY

Source detection and photometry were carried out using SExtractor (Bertin & Arnouts 1996). We constructed a $ch2$ selected catalog by using the dual-image mode capabilities of SExtractor. In dual-image mode, sources are detected and their centroids and apertures are defined in one image and subsequently the photometry is measured in another image using those predetermined apertures and source centers. As in Eisenhardt et al. (2010), the choice of using $ch2$ to construct this catalog was motivated by the fact that cool brown dwarfs are generally brighter in $ch2$ than $ch1$. Photometry was measured in $6\farcs0$ diameter apertures and corrected using the calibration values determined by the IRAC instrument team, -0.133 and -0.113 for $ch1$ and $ch2$, respectively. We use the IRAC zero points provided by the *Spitzer* Science Center (SSC), which are 18.789 and 18.316 Vega magnitudes for $ch1$ and $ch2$, respectively. SExtractor was configured to define a source as a set of 20 or more connected pixels, each lying 1.0σ above the background. We utilize the post-BCD coverage maps to provide an exposure flag (COVCH#) for all sources in the full catalog, with COVCH# equal to the number of frames going into the post-BCD stack at that position. We also provide the SExtractor parameter CLASS_STAR to aid in separating point sources from extended sources. We compared the SExtractor aperture magnitudes for our brown dwarf candidates to an independent measurement of aperture photometry as presented in Kirkpatrick et al. (2011, 2012). This independent photometry tool was written in IDL using both public scripts from IDL Astronomy User's Library[14] and proprietary code created specifically for this task. In short, this IDL code centroids on the known position of the brown dwarf candidate, obtains the aperture photometry of the source, and applies the appropriate aperture corrections as provided by the SSC. We find a mean offset $\Delta\ ch2 \sim 0.001$ mag and a standard deviation sigma ($\Delta\ ch2$) ~ 0.04 mag between the two codes, indicating that both are behaving reasonably.

4. THE CATALOGS

There are three separate catalogs presented in this paper. The first (WISE-Spitzer_BD_photometric_catalog_V1.0.fits in the online journal), described in Section 4.1 and Table 1, is a list of *Spitzer* and *WISE* photometry for 1510 *WISE*-selected brown dwarf candidates targeted in *Spitzer* programs 70062 and 80109. The second (WISE-Spitzer_EXGAL_photometric_catalog_V1.0.fits in the online journal), described in

[13] http://wise2.ipac.caltech.edu/docs/release/allsky

[14] http://idlastro.gsfc.nasa.gov/

Table 1
Brown Dwarf Photometric Catalog Parameters

Parameter	Example Value	Description
DESIGNATION	205628.91+145953.2	*WISE* sexigesimal designation
SPTYPE	Y0	Near-IR Spectral Type
R.A.	314.12046	Right ascension in decimal degrees J2000
DECL.	14.998111	Declination in decimal degrees J2000
CH1MAG	15.873	3.6 μm Vega magnitude
CH1ERR	0.017	3.6 μm Vega magnitude error
CH2MAG	13.914	4.5 μm Vega magnitude
CH2ERR	0.003	4.5 μm Vega magnitude error
W1MPRO	18.253	*WISE* 3.4 μm profile-fit magnitude
W1SIGMPRO	0.000	*WISE* 3.4 μm profile-fit magnitude error
W1SNR	−0.300	*WISE* 3.4 μm signal-to-noise ratio
W2MPRO	13.928	*WISE* 4.6 μm profile-fit magnitude
W2SIGMPRO	0.046	*WISE* 4.6 μm profile-fit magnitude error
W2SNR	23.400	*WISE* 4.6 μm signal-to-noise ratio
W3MPRO	12.003	*WISE* 12.0 μm profile-fit magnitude
W3SIGMPRO	0.270	*WISE* 12.0 μm profile-fit magnitude error
W3SNR	4.000	*WISE* 12.0 μm signal-to-noise ratio
W4MPRO	8.781	*WISE* 22.0 μm profile-fit magnitude
W4SIGMPRO	NaN	*WISE* 22.0 μm profile-fit magnitude error
W4SNR	0.800	*WISE* 22.0 μm signal-to-noise ratio

Note. When W#SIGMPRO is either 0.000 or NaN, it is the same as null in the *WISE* All-sky Source Catalog, see http://wise2.ipac.caltech.edu/docs/release/allsky.

Table 2
W1W2-dropout Photometric Catalog Parameters

Parameter	Example Value	Description
DESIGNATION	000025.1+420708.5	*WISE* sexigesimal designation
R.A.	0.10475330	Right ascension in decimal degrees J2000
DECL.	42.119005	Declination in decimal degrees J2000
CH1MAG	16.759	3.6 μm Vega magnitude
CH1ERR	0.039	3.6 μm Vega magnitude error
CH2MAG	15.837	4.5 μm Vega magnitude
CH2ERR	0.022	4.5 μm Vega magnitude error
W1MPRO	17.912	*WISE* 3.4 μm profile-fit magnitude
W1SIGMPRO	0.241	*WISE* 3.4 μm profile-fit magnitude error
W1SNR	4.500	*WISE* 3.4 μm signal-to-noise ratio
W2MPRO	16.198	*WISE* 4.6 μm profile-fit magnitude
W2SIGMPRO	0.176	*WISE* 4.6 μm profile-fit magnitude error
W2SNR	6.200	*WISE* 4.6 μm signal-to-noise ratio
W3MPRO	11.474	*WISE* 12.0 μm profile-fit magnitude
W3SIGMPRO	0.114	*WISE* 12.0 μm profile-fit magnitude error
W3SNR	9.500	*WISE* 12.0 μm signal-to-noise ratio
W4MPRO	7.50	*WISE* 22.0 μm profile-fit magnitude
W4SIGMPRO	0.092	*WISE* 22.0 μm profile-fit magnitude error
W4SNR	11.800	*WISE* 22.0 μm signal-to-noise ratio

Note. When W#SIGMPRO is either 0.000 or NaN, it is the same as null in the *WISE* All-sky Source Catalog, see http://wise2.ipac.caltech.edu/docs/release/allsky.

Section 4.2 and Table 2, is a list of *Spitzer* and *WISE* photometry for 906 *WISE*-selected HyLIRG candidates (hereafter "W1W2-dropouts"; Eisenhardt et al. 2012) that were the targets for *Spitzer* programs 70162 and 80033. The third (WISE-Spitzer_combined_catalog_V1.0.fits in the online journal), described in Section 4.3 and Table 3, is a list of *all* (COV $\geqslant$ 3) sources found on the *Spitzer* IRAC images for the three programs above.

4.1. The Brown Dwarf Catalog

Brown dwarf candidates were selected from the *WISE* source databases using the color criteria discussed in Kirkpatrick et al. (2011, 2012). To summarize, our main selection used a color cut chosen to select cold brown dwarfs with types $\geqslant$T5. A color cut of $W1-W2 > 1.5$ mag was used with *WISE* internal source lists from early processing runs and $W1-W2 > 2.0$ mag was used for later processing, specifically using the combination of the *WISE* All-Sky Source Catalog and *WISE* All-Sky Reject Table that are contained in the *WISE* All-Sky Data Release (Cutri et al. 2012). We also performed another cut with a much more relaxed color criterion ($W1-W2 > 0.4$ mag) to select bright (W2 S/N > 30), nearby brown dwarfs with types $\geqslant$L5. Other constraints, including the lack of a positional match in earlier-epoch all-sky surveys (2MASS, DSS1, DSS2), cuts on the $W2-W3$ color, stipulations on the reduced χ^2 value from point-spread function photometric fitting, etc., were also imposed, as discussed in Kirkpatrick et al. (2011, 2012).

Table 3
Spitzer Photometric Catalog Parameters

Parameter	Example Value	Description
AOR_KEY	r40819456	Astronomical Observation Request
SURVEY	BD	Origin of *Spitzer* follow-up (BD or EXGAL)
R.A.	332.35145	Right ascension in decimal degrees (J2000)
DECL.	−27.565469	Declination in decimal degrees (J2000)
CH1MAG	14.183	3.6 μm Vega magnitude
CH1ERR	0.003	3.6 μm Vega magnitude error
CH2MAG	14.147	4.5 μm Vega magnitude
CH2ERR	0.003	4.5 μm Vega magnitude error
CLASS_STAR_CH1	0.930	SExtractor star–galaxy separator measured 3.6 μm
CLASS_STAR_CH2	0.950	SExtractor star–galaxy separator measured at 4.5 μm
COVCH1	5	Total number of *Spitzer* frames at source position 3.6 μm
COVCH2	5	Total number of *Spitzer*frames at source position 4.5 μm
W1MPRO	14.192	*WISE* 3.4 μm profile-fit magnitude
W1SIGMPRO	0.032	*WISE* 3.4 μm profile-fit magnitude error
W1SNR	34.000	*WISE* 3.4 μm signal-to-noise ratio
W2MPRO	14.203	*WISE* 4.6 μm profile-fit magnitude
W2SIGMPRO	0.056	*WISE* 4.6 μm profile-fit magnitude error
W2SNR	19.400	*WISE* 4.6 μm signal-to-noise ratio
W3MPRO	12.661	*WISE* 12.0 μm profile-fit magnitude
W3SIGMPRO	NaN	*WISE* 12.0 μm profile-fit magnitude error
W3SNR	−0.3000	*WISE* 12.0 μm signal-to-noise ratio
W4MPRO	9.0360	*WISE* 22.0 μm profile-fit magnitude
W4SIGMPRO	NaN	*WISE* 22.0 μm profile-fit magnitude error
W4SNR	0.100	*WISE* 22.0 μm signal-to-noise ratio
JMAG	15.304	2MASS *J* magnitude
JERR	0.055	2MASS *J* magnitude error
HMAG	14.635	2MASS *H* magnitude
HERR	0.063	2MASS *H* magnitude error
KMAG	14.471	2MASS K_s magnitude
KERR	0.083	2MASS K_s magnitude error
BMAG	19.690	USNO-B *B*2 magnitude
RMAG	18.370	USNO-B *R*2 magnitude

Note. When W#SIGMPRO is either 0.000 or NaN, it is the same as null in the *WISE* All-sky Source Catalog, see http://wise2.ipac.caltech.edu/docs/release/allsky.

Most of the selected sources were scheduled for *Spitzer* $ch1$ and $ch2$ observations as part of programs 70062 and 80109. As of late 2012 May, a total of 1564 unique candidates had been observed in both IRAC bands. We were not able to identify a *Spitzer* counterpart for 54 of these candidates, which were therefore deemed to be spurious sources in *WISE*. Further inspection revealed that these spurious sources fell into two categories: (1) cosmic rays that bled through to the final images in the *WISE* co-addition process due to multiple cosmic-ray hits and low frame coverage and (2) *WISE* sources within nebulous patches (or nebulae themselves) rather than nearby brown dwarfs. For the remaining 1510 candidates, however, *Spitzer* counterparts were easily detected in both $ch1$ and $ch2$ bands. These 1510 sources comprise the *WISE*-selected Brown Dwarf Photometric Catalog, as described in Table 1.

The *WISE* and *Spitzer* photometry for each source in this catalog is graphically illustrated in Figure 1. This figure plots the *Spitzer*/IRAC $ch1 - ch2$ color as a function of *WISE* $W1 - W2$ color. The 1510 sources from the catalog are shown by black dots. A total of 166 of these have spectroscopic confirmation from Mainzer et al. (2011), Burgasser et al. (2011), Kirkpatrick et al. (2011, 2012), Cushing et al. (2011), and G. Mace et al. (in preparation), and are plotted with colored symbols, as indicated in the legend of the plot. The coldest brown dwarfs, the Y dwarfs, populate the reddest locus. The location of our latest type Y dwarf, WISE J182831.08+265037.7, which was targeted in a different *Spitzer* program (program 551; PI: Mainzer), is shown by the magenta octagon. As further illustrated in Figure 8 of Kirkpatrick et al. (2012), the *Spitzer* $ch1 - ch2$ color for WISE 1828+2650, typed as $\geqslant$Y2, is not as red as objects typed slightly earlier, at Y1.

Many excellent brown dwarf candidates in the catalog and on this diagram still lack spectroscopic data. Of the five objects in Figure 1 with colors of $ch1 - ch2 > 2.8$ mag, three are promising Y dwarf candidates—WISE J064723.23−623235.5 ($ch1 - ch2 = 2.87$, $W1 - W2 > 3.77$), WISE J082507.35+280548.5 ($ch1 - ch2 = 2.96$, $W1 - W2 > 3.75$), and WISE J220905.73+271144.00 ($ch1 - ch2 = 2.98$, $W1 - W2 > 3.68$). All three are extremely faint in the *J* and *H* passbands, so we are awaiting spectroscopic confirmation using the WFC3 grisms on board the *Hubble Space Telescope*. The other two sources, WISE 035358.23+375458.5 ($ch1 - ch2 = 3.00$, $W1 - W2 = 3.52$) and WISE J141127.45−612925.6 ($ch1 - ch2 = 3.42$, $W1 - W2 > 3.35$), are located within nebular patches on the *Spitzer* images and appear to be reddened or embedded objects rather than brown dwarfs.

These last two sources highlight an important point: spectroscopic confirmation of sources is vital to establishing candidates as bona fide brown dwarfs. Sixteen of our targets, shown by the yellow dots in Figure 1, have been shown spectroscopically *not* to be brown dwarfs (G. Mace et al. in preparation).

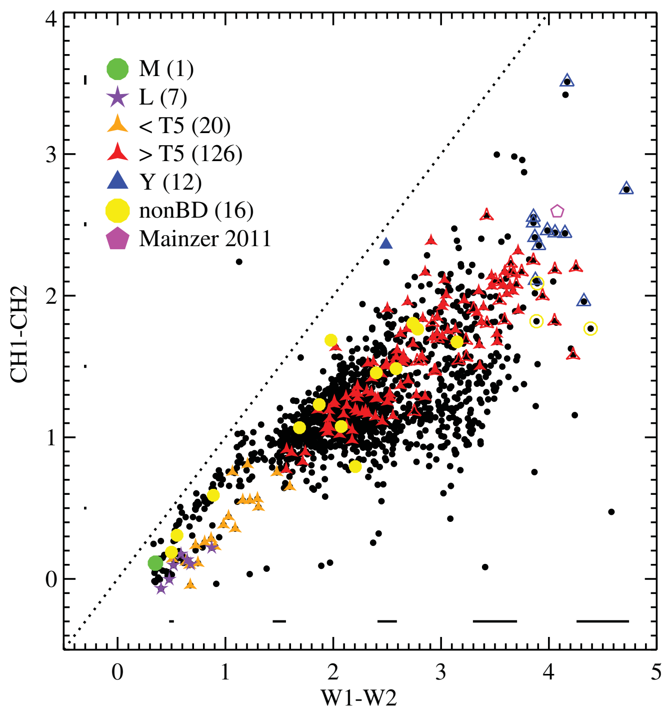

Figure 1. *Spitzer*/IRAC $ch1 - ch2$ as a function of $W1 - W2$ color. Black points are observations of 1510 *WISE*-selected brown dwarfs detected by *Spitzer*. Those with spectroscopic classifications are overplotted in color, described in the legend. Open symbols denote color limits in $W1 - W2$. We present the median uncertainties in each full magnitude bin of color for both axes and these are shown as the tick marks along the lower and left axes. The dotted line represents the one-to-one relationship between the axes.

(A color version of this figure is available in the online journal.)

These scatter widely over the diagram, proving that there is contamination at all colors. One interesting feature can be seen in the lower left quadrant of the diagram where our L and early-T dwarf candidates lie. These objects have bright *WISE* and *Spitzer* magnitudes, so the colors of these objects are well measured. These high-quality measurements enable us to split objects with $W1 - W2 < 1.5$ mag and $ch1 - ch2 < 1.0$ mag into two tracks. The lower track is replete with spectroscopically confirmed L and early-T dwarfs and primarily have 2MASS detections; the upper track has fewer confirming observations and generally no 2MASS detections, but objects with spectra here are typically not found to be brown dwarfs. Users of this catalog are cautioned that the sources here are candidates only, our selections were fairly liberal, so contamination by other types of sources is expected.

4.2. The W1W2-dropout Catalog

Eisenhardt et al. (2012) have identified a rare population of objects termed "$W1W2$-dropout" galaxies, because they are faint or undetected in $W1$ and $W2$ but well detected in $W3$ or $W4$. Optical spectroscopy shows that most of these objects have redshift $z > 1.6$ (Eisenhardt et al. 2012), which in combination with submillimeter follow-up detections results in bolometric luminosities $>10^{13}\ L_\odot$ and in some cases $>10^{14}\ L_\odot$ (Wu et al. 2012). This qualifies them as HyLIRGs, the other primary science objective for *WISE* (the first being cool brown dwarfs, as noted in the introduction). The submillimeter data show that their luminosities are dominated by dust with temperatures more than twice as high as other infrared luminous populations, which leads Wu et al. (2012) to refer to them as hot dust obscured galaxies or "hot DOGs." A closely related population shows a high incidence (1/3) of very extended (>30 kpc) Lyα emission or Lyα blobs, which normally are found in less than 1% of galaxies, as described in Bridge et al. (2012). The extreme luminosities, hot dust, and prevalence of Lyα blobs in this population suggest they may be a rare phase in the co-evolution of galaxies and their central supermassive black holes.

Approximately 1000 $W1W2$-dropouts have been identified in the *WISE* catalog, and because of their faintness in W1 and W2, 919 have been followed up in the *Spitzer* IRAC $ch1$ and $ch2$ bands. Of the 919 sources, 910 were selected in *Spitzer* cycle 7, 9 were added in cycle 8, and 13 failed to meet the SExtractor detection thresholds described in Section 3.

The IRAC $ch1$ and $ch2$ bands are similar in wavelength to W1 and W2 but can easily reach much greater depths. These bands sample near-infrared wavelengths in the rest frame at the typical $z \sim 2$ of $W1W2$-dropouts, providing a measure of the stellar population in the galaxies. Figure 1 of Eisenhardt et al. (2012) shows the resulting distribution of $ch1 - ch2$ colors converted to $W1 - W2$. Here, we present (in Table 2) *Spitzer* and *WISE* photometry for the 906 sources detected in the *Spitzer* data by SExtractor.

The bulk of the $ch1 - ch2$ colors lie well above $W1 - W2 = 0.8$, which indicates that the source has a high probability of being an active galactic nucleus (AGN), as Stern et al. (2012) show. The optical spectra also often show AGN signatures (Wu et al. 2012), and it appears likely that the bulk of their extraordinary luminosity is powered by accretion onto supermassive black holes. As shown in Eisenhardt et al. (2012), the unusually high ratio of $W3$ and $W4$ emission relative to $ch1$ suggests a higher ratio of supermassive black hole mass to stellar mass than is found in local galaxies, implying the black holes grow before their stellar populations. This sequence is unexpected in the most frequently discussed scenarios of galaxy and AGN feedback (e.g., Hopkins 2012).

4.3. The Complete Photometric Catalog

We provide a catalog of the $\sim 7.33 \times 10^5$ sources found in the *Spitzer* fields (COVCH1 $\geqslant$ 3 and COVCH2 $\geqslant$ 3) whose properties are described in Table 3. We provide *WISE* and 2MASS photometry from the *WISE* All-Sky source catalog for sources that fall within 2″ of a *Spitzer* source. In addition, we provide optical photometry for *Spitzer* sources that fall within 2″ of a source in the USNO-B catalog. Table 4 summarizes the statistics that resulted from matching between these catalogs for two different samples. Sample A comprises sources with the deepest imaging and most reliable photometric measurements available (COVCH1 = 5 and COVCH2 = 5). Sample B represents sources with slightly shallower imaging (COVCH1 $\geqslant$ 3 and COVCH2 $\geqslant$ 3) and thus slightly lower photometric reliability, though still reasonably good enough for most scientific purposes.

To characterize the photometric sample, we provide color–color and color–magnitude diagrams in Figure 2. The left plot of Figure 2 is similar to Figure 1, but includes all sources from Sample A having *WISE* measurements (a total of $\sim 10^5$ sources) rather than just the *WISE* brown dwarf candidates. We also show these colors for the 166 spectroscopically confirmed brown dwarfs, plotted with colored symbols as indicated in the legend of the plot. Few field sources in the *Spitzer* images have colors as extreme as the latest T and Y dwarfs.

In the center plot of Figure 2, we show $ch1 - ch2$ versus $ch2$ mag. The limiting magnitude is $ch2 \sim 18.0$ mag, which is $\sim$2.5 mag fainter then the *WISE*-selected candidates

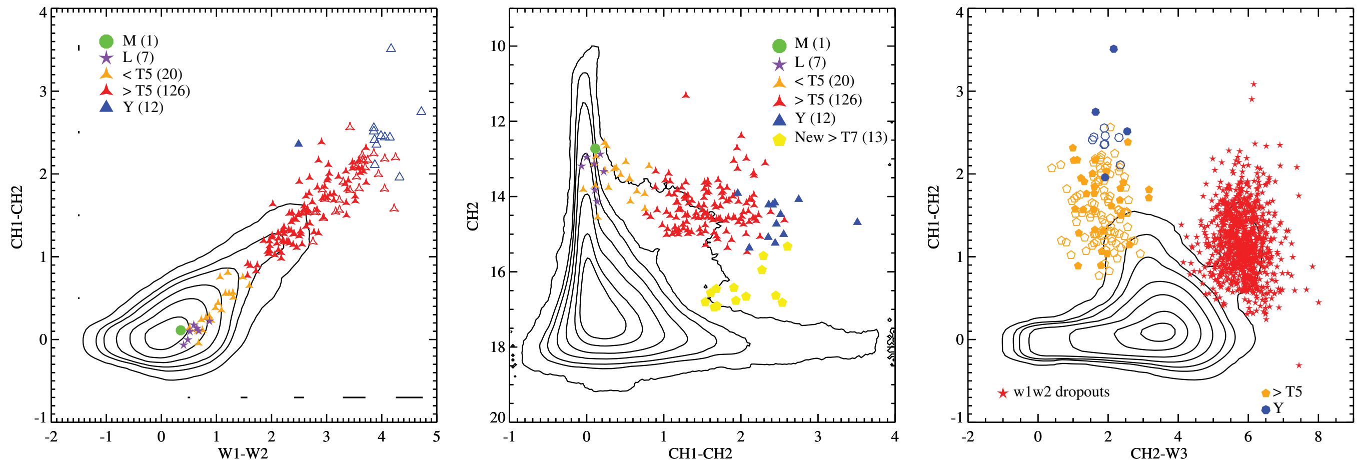

Figure 2. Left: *Spitzer*/IRAC $ch1 - ch2$ as a function of *WISE* $W1 - W2$ color. Contours represent all sources with photometric measurements from these two instruments ($\sim 10^5$ sources). Objects with spectroscopic classification are shown by the colored points. Open symbols denote color limits in $W1 - W2$. Center: *Spitzer*/IRAC $ch1 - ch2$ as a function of $ch2$ magnitude. Contours show $\sim 3.4 \times 10^5$ sources (sample A in Table 4). Objects with spectroscopic classification are shown by the colored points. We also show the 13 newly discovered candidates as yellow circles. Right: *Spitzer*/IRAC $ch1 - ch2$ as a function of $ch2 - W3$ color. Contours are similar to the left plot. Brown dwarfs with spectroscopic classification greater than T5 are shown in orange (T) and blue (Y). We also present the *WISE*-selected HyLIRG candidates in red. Open symbols denote color upper limits. The contours represent the 40, 60, 80, 90, 95, 97, and 99 percentiles of the distribution. Tick marks along the axes of the left panel are computed as discussed in Figure 1.

(A color version of this figure is available in the online journal.)

Table 4
Photometric Catalog Statistics

Sample	Coverage	No. of w/*Spitzer*	No. of w/*WISE*	No. of w/2MASS	No. of w/USNO-B
A	=5	3.41×10^5	1.00×10^5	3.90×10^4	7.75×10^4
B	$\geqslant 3$	7.33×10^5	2.02×10^5	8.22×10^4	1.63×10^5

and comparable to the depth of the IRAC Shallow Survey (Eisenhardt et al. 2004), which had similar exposure time. We see that the majority of the *WISE*-selected brown dwarf candidates occupy a diffuse region in this color–magnitude domain, mainly with $ch2 < 15.5$ and $ch1 - ch2 > 0.7$.

It is challenging to separate Galactic sources from extragalactic sources using the $ch1$ and $ch2$ filters in the IRAC camera alone. In the rightmost plot of Figure 2, we show $ch1 - ch2$ versus $ch2 - W3$. Here, we can see the benefit of including photometric measurements at 12 μm. The additional color information helps separate the Galactic and extragalactic red ($ch1 - ch2 > 1$) populations with cool brown dwarfs having $ch2 - W3 < 3$, while the extragalactic population has $ch2 - W3 > 3$. A similar separation is shown in Figure 1 of Eisenhardt et al. (2010).

5. NEW BROWN DWARF CANDIDATES SELECTED FROM *SPITZER*

We present new brown dwarf candidates discovered from a blind search using the following search criteria: $ch1 - ch2 \geqslant 1.5$, $ch2 \leqslant 17.0$ mag and coverage equal to 5 in both IRAC channels (sample A from Table 4). As noted by Eisenhardt et al. (2010), this choice of color is expected for sources with spectral types later than T7 and the magnitude cut allows for only robustly measured sources to be inspected. This search resulted in 666 candidates from the brown dwarf fields and 247 candidates from the extragalactic fields. We then used the basic calibrated data (BCDs) to inspect the individual frames to remove any spurious sources or sources which appeared to be contaminated by cosmic rays. After also removing sources which were the *WISE*-selected targets, we were left with 13 new ultra-cool brown dwarf candidates: seven in the *WISE* brown dwarf fields and six in the *WISE* HyLIRG fields. Table 5 lists these 13 candidates, and Multi-wavelength finder charts ($1' \times 1'$) for them are presented in Figure 3. The finder charts show that all of these candidates lack detections at shorter wavelengths and 12 μm, as expected for brown dwarf candidates. However, the *Spitzer* images are relatively deep compared to the observations at shorter (DSS, 2MASS) and longer wavelengths (*WISE*). The difference in depth between these sets of observations makes it difficult to exclude certain types of extra-galactic objects such as AGNs.

For comparison, Eisenhardt et al. (2010) found 32 similar brown dwarf candidates in the deeper Spitzer Deep Wide Field Survey (SDWFS; Ashby et al. 2009) covering 10 deg^2, but selecting candidates to a fainter limit, $ch2 \leqslant 18.5$. Of these 32 SDWFS brown dwarf candidates, 7 had $ch2 \leqslant 17.0$. After accounting for the coverage depth of 5 criterion, the 2483 IRAC pointings searched here cover a comparable area to SDWFS, suggesting a somewhat higher surface density of brown dwarfs candidates than in SDWFS. All of the SDWFS candidates with $ch2 \leqslant 17.0$ were among those rejected as probable AGNs because they had $ch2 - ch4 > 2$. An analogous AGN rejection criterion using the $ch2 - W3$ color is not possible here because the $W3$ depth is not adequate, so it is plausible that many of the 13 brown dwarf candidates identified here are AGNs. If so, then it is possible that the somewhat higher surface density is attributable to AGN clustering.

Determining whether any of the new candidates could potentially be widely separated companions can be achieved in two ways. First, we check the surface density of our brown dwarf candidates in the control sample versus that in the brown dwarf fields. We find a surface density of (1.5 ± 0.6 deg^{-2}) in the

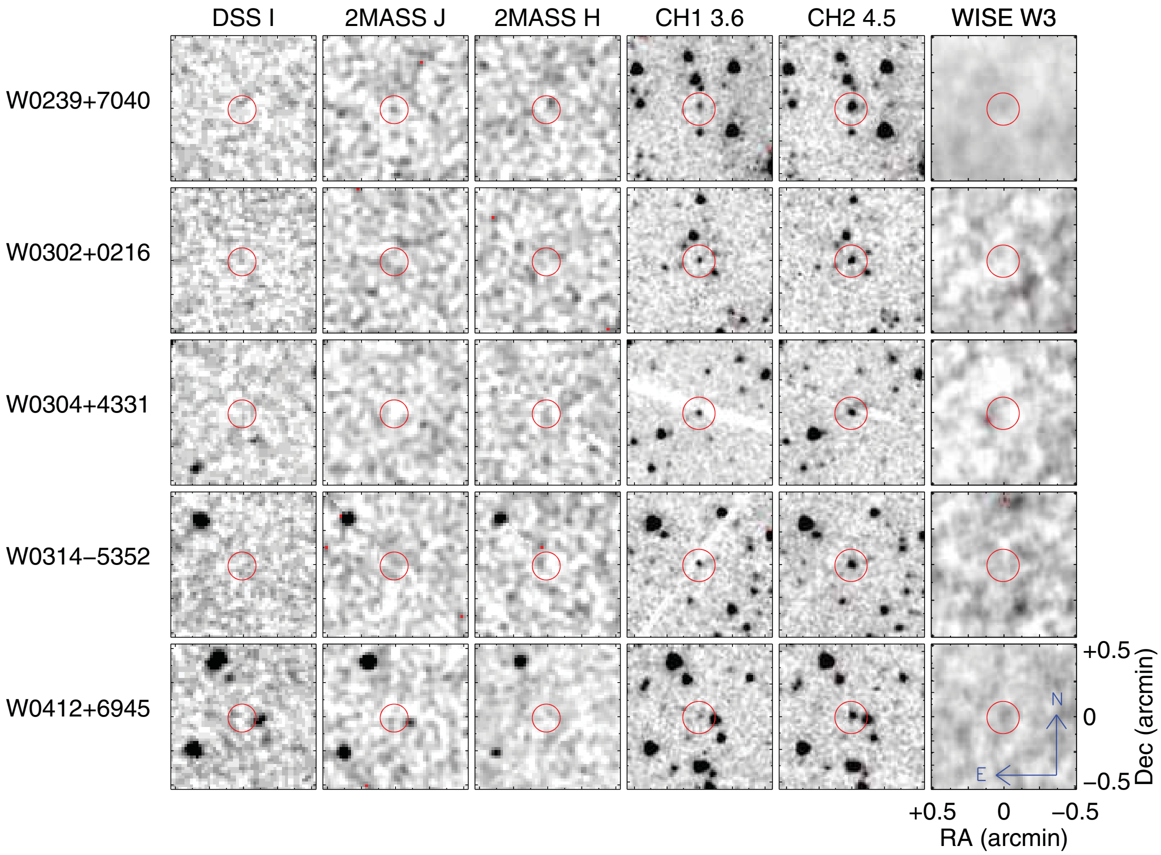

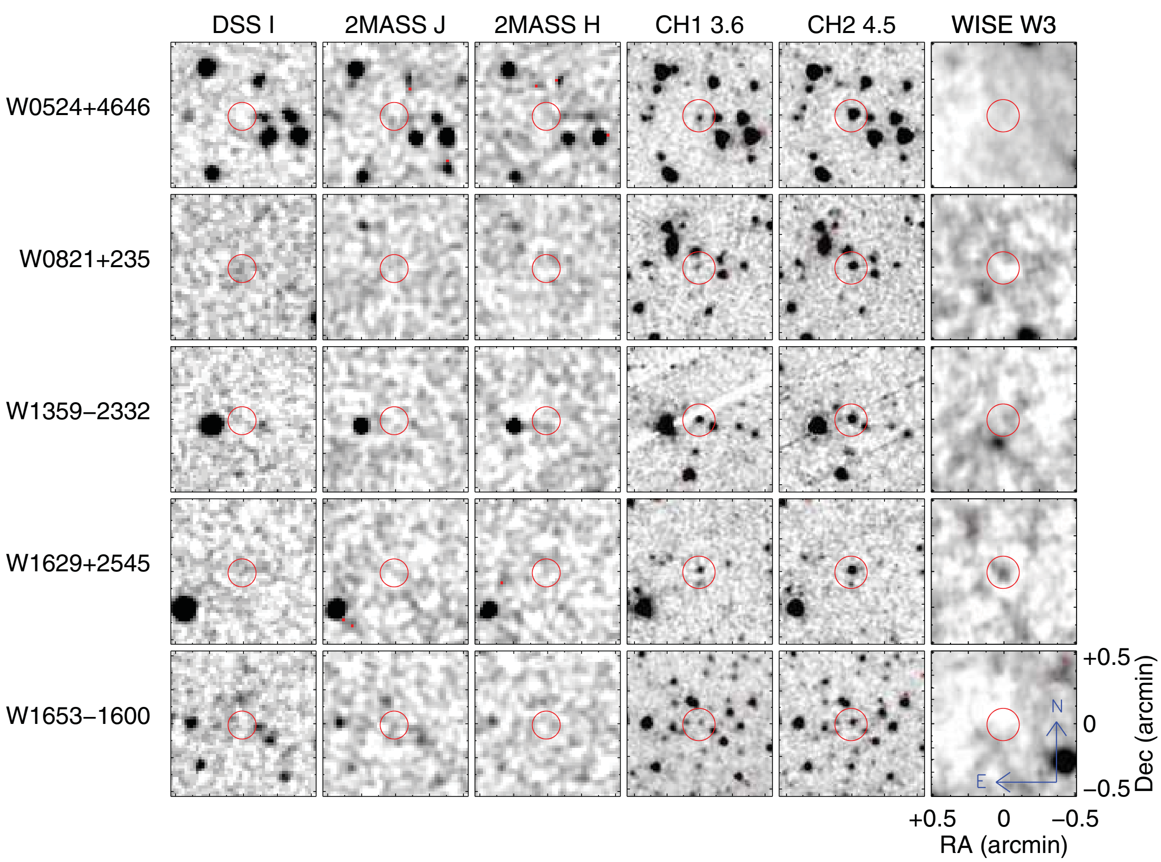

Figure 3. Multi-wavelength finder charts for the new ultra-cool brown dwarf candidates. We present 1×1 arcminute cutouts from various all-sky surveys alongside the *Spitzer* discovery images. From left to right, these cutouts are from the Digitized Sky Survey *I* band, 2MASS *J* and *H*, *Spitzer ch*1 and *ch*2, and *WISE W*3. The images are oriented with north up and east to the left.

(A color version of this figure is available in the online journal.)

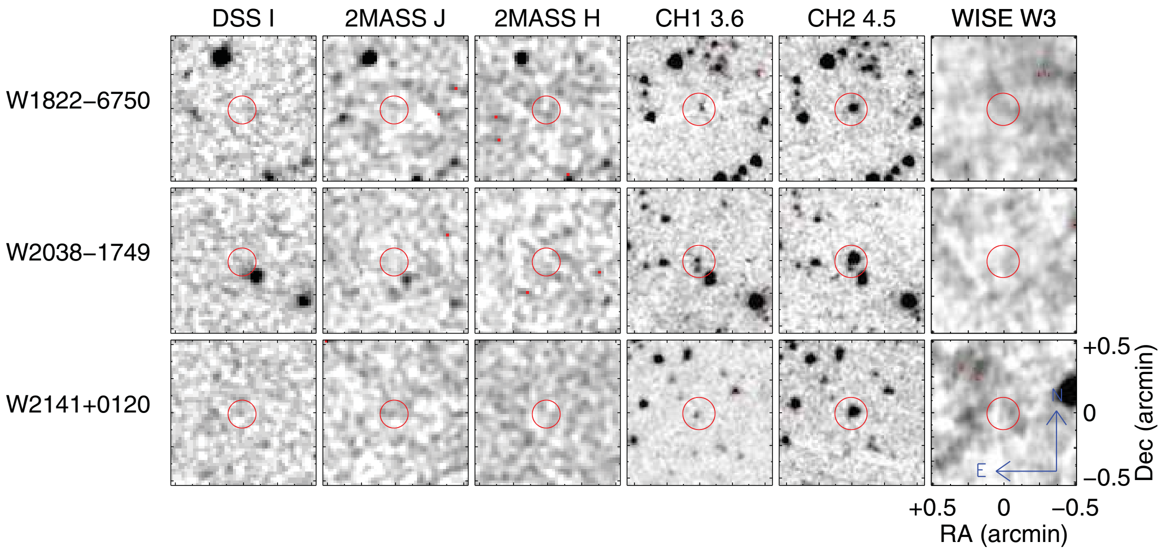

Figure 3. (Continued)

control sample and (1.0 ± 0.4 deg^{-2}) in the brown dwarf fields. The errors are calculated based on simple Poisson statistics. The fact that the control field has a larger surface density suggests that the candidates found are unlikely to be physically associated companions. Second, we can determine the spectrophotometric distances to both the primary *WISE*-selected source and the new *Spitzer*-selected candidate. We estimate the spectral type by using Figure 11 from Kirkpatrick et al. (2011) and the derived $ch1 - ch2$ color. We then estimate the photometric distances listed in Table 5 using the apparent magnitude and the absolute magnitude, where the latter is estimated using the absolute magnitude versus spectral type relationship in Figure 13 of Kirkpatrick et al. (2012).

Most of the new candidates do not appear to be physically associated with the *WISE*-selected targets, but are more distant background sources. Assuming that the *WISE*-selected candidates are indeed brown dwarfs, they reside at ~20 pc, while the majority of the new *Spitzer*-selected candidates are at $\gtrsim$40 pc. There is only one case for which both the primary and the candidate may be physically associated, J052439.3+464631.2, where both sources have estimated distances of ~20 pc. The estimated spectral types for these two sources are T6 and T9. The angular separation of 83$''\!.$26 for this system corresponds to a physical separation of at least 1600 AU at 20 pc.

The probability of discovering widely separated companions rests on the probability that such systems exist, which is itself a complicated function of mass, age, environment, and formation mechanisms. An in depth review on multiplicity in very low mass systems is given in Burgasser et al. (2007) and references therein. These brown dwarf primaries have low mass and thus small gravitational potential wells. This is well summarized in Figure 6 of Burgasser et al. (2007), where they plot the separation of binaries as a function of total mass for a wide variety of known systems. Brown dwarf binaries tend to have small separations with higher binding energies. Systems with lower binding energies tend to be disrupted, primarily due to outside perturbers or gravitational instabilities, which translates to almost no old brown dwarf binaries having been found with separations greater than 20 AU. There are only a handful of low-mass binaries with separations greater than 20 AU, three are relatively young and thus have not had enough time for collisional disruption. Another system is DENIS 0551-4443AB (Billères et al. 2005), which is thought to be relatively old and is the kind of widely separated system for which we were searching. Billères et al. (2005) suggest that such a system is fragile, and it would not have survived a close encounter with a third body. Furthermore, its existence demonstrates that some very low mass stars/brown dwarfs form without ejection from a multiple system, or any other strong dynamical interaction. Other widely separated multiple systems have been discovered since Burgasser et al. (2007), including the NLTT20346 + 2MASS J0850359+105716 system (Faherty et al. 2011). Is it possible that J052439.3+464631.2 is also an old, widely separated binary like these?

The nature of J052439.3+464631.2 can be probed further by considering the environment, magnitudes, and colors of the individual objects in this system. Using the *WISE* All-Sky Image Archive, we investigate a region ~5′ on a side centered on the new candidate and make the following observations. First, this system resides near the Galactic Plane which makes it more difficult to interpret given the high source density and complex nebulosity. The pair resides at the edge of a 12 μm bright nebula, thus suggesting that rather than a widely separated T6–T9 binary, these are more likely reddened or embedded objects and not brown dwarfs. Another possibility is that they could be physically associated T6 and T9 brown dwarfs, though not in a binary system, i.e., forming in the same stellar cocoon and around the same time. Spectroscopic observations of these candidates should be made to disentangle these scenarios.

Other than J052439.3+464631.2, this search yielded no plausible widely separated companions, therefore suggesting that very low mass (>T7) brown dwarf binaries with separations of 20 to 2000 AU are extremely rare.

6. SUMMARY

This paper summarizes initial *Spitzer* follow-up and analysis of some of the rarest astrophysical objects discovered to date. We present, for the first time, a very large sample of *WISE*-selected ultra-cool brown dwarf candidates. Of these, 184 have spectroscopic data with ~92% of them confirmed as bona fide ultra-cool brown dwarfs and of which ~83% have spectral types later than T5. We also present 13 new, though more distant, ultra-cool (>T7) brown dwarf candidates discovered using the *Spitzer* data. Only one possible widely separated companion

Table 5
New Brown Dwarf Candidates

Origin	Candidate		Candidate		Primary		Type[a]	Type[b]	d_{est}[c]	d_{est}[d]	Separation[e]
	R.A. (J2000)	Decl. (J2000)	*ch*2	*ch*1 − *ch*2	*ch*2	*ch*1 − *ch*2			(pc)	(pc)	
BD	02:39:59.8	+70:40:20.4	16.42 ± 0.04	1.91 ± 0.16	14.14 ± 0.01	0.78 ± 0.01	T8	T5	40.6	21.8	36.″27
EXGAL	03:02:21.1	02:16:09.8	16.80 ± 0.05	1.54 ± 0.18							
EXGAL	04:12:09.3	69:45:24.1	16.94 ± 0.06	1.65 ± 0.22							
BD	05:24:39.3	+46:46:31.2	15.57 ± 0.02	2.29 ± 0.11	14.52 ± 0.01	1.03 ± 0.01	T9	T6	20.5	21.5	83.″26
EXGAL	08:21:51.3	23:45:17.1	16.63 ± 0.04	2.45 ± 0.32							
BD	16:29:50.0	+25:45:25.9	16.45 ± 0.03	1.68 ± 0.12	15.44 ± 0.01	1.06 ± 0.03	T7.5	T6	44.5	32.8	139.″13
BD	16:53:42.8	−16:00:10.0	16.91 ± 0.08	1.69 ± 0.33	14.61 ± 0.01	1.00 ± 0.02	T7.5	T5.5	54.92	24.1	44.″98
EXGAL	20:38:38.1	−17:49:49.1	15.32 ± 0.01	2.61 ± 0.12							
EXGAL	21:41:45.5	01:20:14.5	15.95 ± 0.02	2.27 ± 0.19							
EXGAL	03:14:52.0	−53:52:41.9	16.81 ± 0.04	2.54 ± 0.40							
BD	03:04:26.6	+43:31:10.9	16.77 ± 0.05	1.93 ± 0.22	14.90 ± 0.01	1.22 ± 0.02	T8	T7	47.6	23.0	21.″38
BD	18:22:38.6	−67:50:03.9	16.66 ± 0.04	2.06 ± 0.22	15.12 ± 0.01	1.09 ± 0.02	T9	T6.5	33.9	26.7	96.″27
BD[f]	13:59:42.7	−23:32:35.6	16.56 ± 0.04	1.61 ± 0.16			T7				

Notes.
[a] Estimated brown dwarf type for new candidate.
[b] Estimated brown dwarf type for primary.
[c] Estimated distance to the new candidate, in parsecs.
[d] Estimated distance to the primary, in parsecs.
[e] Distance between new candidate and the primary, in arcseconds.
[f] primary *Spitzer* target for this observation was not detected in the imaging, thus no information is given for the primary target.

system was found, suggesting that widely separated, cold brown dwarf binaries are extremely rare. To date, the *WISE* team has only followed up a small percentage (∼12%) of the total *WISE*-selected sample, providing follow-up opportunities by the astrophysical community on a host of interesting discoveries yet to be made. Given the wide range of (sub)stellar spectral types it probes, the sample will allow for a multitude of future statistical studies. In addition, this sample will provide excellent follow-up sources for the *James Webb Space Telescope*.

There are several avenues of investigation yet to be fully explored which we summarize as follows. Detailed proper motion measurements can be made with the current data available (*WISE* + *Spitzer*), though long term monitoring will allow for full kinematics and robust distances to be determined. Several large parallax programs are currently underway monitoring a large number of the spectroscopically verified sources, though many remain to be monitored. Long term monitoring will also provide critical insight and constraints on variability in brown dwarfs, two examples being the study of atmospheric meteorology and possible detection of transits by planetary companions. Using the difference between the *WISE* and *Spitzer* filter profiles will allow one to explore differences in the underlying spectra at these wavelengths. With no all-sky deep surveys planned at these wavelengths in the foreseeable future, this is the quintessential brown dwarf sample because it comprises the closest and brightest brown dwarfs possible.

In addition to presenting these two very rare populations of astrophysical sources, we release a catalog of $\sim 7.33 \times 10^5$ objects detected in the *Spitzer* observations, including multi-wavelength (2MASS, USNO-B, and *WISE*) photometry for a subsample. Providing multi-wavelength photometry for hundreds of thousands of astrophysical sources will allow for a number of scientific studies to be conducted, from fully characterizing the mid-IR properties of the coldest brown dwarfs, to a more complete characterization of the most IR luminous galaxies in the universe.

This publication makes use of data products from the *Wide-Field Infrared Survey Explorer*, which is a joint project of the University of California, Los Angeles, and the Jet Propulsion Laboratory/California Institute of Technology, funded by the National Aeronautics and Space Administration (NASA). This publication also makes use of observations made with the *Spitzer Space Telescope*, which is operated by the Jet Propulsion Laboratory, California Institute of Technology, under a contract with NASA. This work is also based in part on observations made with the NASA/ESA *Hubble Space Telescope*, obtained at the Space Telescope Science Institute, which is operated by the Association of Universities for Research in Astronomy, Inc., under NASA contract NAS 5-26555. Some of the spectroscopic classifications presented herein were obtained at the W. M. Keck Observatory, which is operated as a scientific partnership among the California Institute of Technology, the University of California and the National Aeronautics and Space Administration. This publication also makes use of data products from 2MASS. 2MASS is a joint project of the University of Massachusetts and the Infrared Processing and Analysis Center/California Institute of Technology, funded by the National Aeronautics and Space Administration and the National Science Foundation. This research has made use of the NASA/IPAC Infrared Science Archive (IRSA), which is operated by the Jet Propulsion Laboratory, California Institute of Technology, under contract with NASA.

REFERENCES

Ashby, M. L. N., Stern, D., Brodwin, M., et al. 2009, ApJ, 701, 428
Bertin, E., & Arnouts, S. 1996, A&AS, 117, 393
Billères, M., Delfosse, X., Beuzit, J.-L., et al. 2005, A&A, 440, L55
Bridge, C. R., et al. 2012, arXiv:1205.4030
Burgasser, A. J. 2008, in ASP Conf. Ser. 384, 14th Cambridge Workshop on Cool Stars, Stellar Systems, and the Sun, ed. G. van Belle (San Francisco, CA: ASP), 126
Burgasser, A. J., Cushing, M. C., Kirkpatrick, J. D., et al. 2011, ApJ, 735, 116

Burgasser, A. J., Reid, I. N., Siegler, N., et al. 2007, in Protostars and Planets V, ed. B. Reipurth, D. Jewitt, & K. Keil (Tucson, AZ: Univ. Arizona Press), 427
Burningham, B., Pinfield, D. J., Lucas, P. W., et al. 2010, MNRAS, 406, 1885
Cushing, M. C., Kirkpatrick, J. D., Gelino, C. R., et al. 2011, ApJ, 743, 50
Cutri, R. M., et al. 2012, Explanatory Supplement to the WISE All-Sky Data Release Products, Technical Report
Eisenhardt, P. R. M., Griffith, R. L., Stern, D., et al. 2010, AJ, 139, 2455
Eisenhardt, P. R., Stern, D., Brodwin, M., et al. 2004, ApJS, 154, 48
Eisenhardt, P. R. M., Wu, J., Tsai, C.-W., et al. 2012, ApJ, 755, 173
Epchtein, N., de Batz, B., Capoani, L., et al. 1997, Messenger, 87, 27
Faherty, J. K., Burgasser, A. J., Bochanski, J. J., et al. 2011, AJ, 141, 71
Fazio, G. G., Hora, J. L., Allen, L. E., et al. 2004, ApJS, 154, 10
Gelino, C. R., Kirkpatrick, J. D., Cushing, M. C., et al. 2011, AJ, 142, 57
Hayashi, C., & Nakano, T. 1963, Prog. Theor. Phys., 30, 460
Hopkins, P. F. 2012, MNRAS, 420, L8
Kirkpatrick, J. D. 2000, in ASP Conf. Ser. 212, From Giant Planets to Cool Stars, ed. C. A. Griffith & M. S. Marley (San Francisco, CA: ASP), 20
Kirkpatrick, J. D. 2005, ARA&A, 43, 195
Kirkpatrick, J. D. 2008, in ASP Conf. Ser. 384, 14th Cambridge Workshop on Cool Stars, Stellar Systems, and the Sun, ed. G. van Belle (San Francisco, CA: ASP), 85
Kirkpatrick, J. D., Cushing, M. C., Gelino, C. R., et al. 2011, ApJS, 197, 19
Kirkpatrick, J. D., Reid, I. N., Liebert, J., et al. 1999, ApJ, 519, 802
Kirkpatrick, J. D., Gelino, C. R., Cushing, M. C., et al. 2012, ApJ, 753, 156
Kumar, S. S. 1963, ApJ, 137, 1121
Mainzer, A., Cushing, M. C., Skrutskie, M., et al. 2011, ApJ, 726, 30
Metchev, S. A., Kirkpatrick, J. D., Berriman, G. B., & Looper, D. 2008, ApJ, 676, 1281
Morgan, W. W., Keenan, P. C., & Kellman, E. 1943, An Atlas of Stellar Spectra, with an Outline of Spectral Classification (Chicago, IL: Univ. Chicago Press)
Reylé, C., Delorme, P., Willott, C. J., et al. 2010, A&A, 522, A112
Skrutskie, M. F., Cutri, R. M., Stiening, R., et al. 2006, AJ, 131, 1163
Stern, D., Assef, R. J., Benford, D. J., et al. 2012, ApJ, 753, 30
Wright, E. L., Mainzer, A., Gelino, C., & Kirkpatrick, D. 2011, arXiv:1104.2569
Wright, E. L., Eisenhardt, P. R. M., Mainzer, A. K., et al. 2010, AJ, 140, 1868
Wu, J., Tsai, C.-W., Sayers, J., et al. 2012, ApJ, 756, 96
York, D. G., Adelman, J., Anderson, J. E., Jr., et al. 2000, AJ, 120, 1579